A GENERAL FOOTPRINT GENERATION APPROACH FOR LIFTING RE-ENTRY VEHICLE

Zhang Rui, Li Zhaoying, Shi Linan
School of Astronautics, Beijing University of Aeronautics and Astronautics, Beijing 100191, China
zhangrui@buaa.edu.cn; lizhaoying@buaa.edu.cn; shi_linan@163.com

Keywords: *re-entry vehicle; footprint; bank angle; trajectory*

Abstract

Footprint is an important index of flight maneuverability for entry vehicle. In this paper the footprint is separated into inner and outer boundaries which are generated based on different methods. It involves algorithms for solving maximum downrange, maximum crossrange, and minimum trajectory problems with the same initial and terminal conditions. Path constraints of heating rate, dynamic pressure and aerodynamic load are considered. Simulation is given and verifies the proposed approach.

1 Introduction

Footprint is the set of all the reachable landing spots of entry vehicles with given initial, path and terminal constraints. It is an important index to evaluate the maneuverability of vehicle.

Footprint problem is an optimal control problem and there are four typical methods by which the footprint has been successfully obtained. The footprint problem is converted into three parameters searching problem for maximum crossrange with free downrange by coordinate transform [1]. The coordinate transform makes the process a little complicate in some sort and path constraints are not considered. It can also be converted into trajectory optimization problem and direct methods such as pseudo-spectral method and direct collocation method are used [2-5]. The direct methods usually have large computation and could not guarantee the convergence even though it needs no optimal necessary condition. The maximum drag profile and minimum drag profile are also used to find the approximately outer and inner boundary of footprint [6,7]. The equivalence of closest approach problem and maximum crossrange at prescribed downrange problem is proved and the footprint is solved through single parameter searching for closest approach problem [8,9]. However, the setting of virtual targets for the closest approach problem was stochastically and the method did not provide a general way to guarantee all the chosen virtual targets were unreachable. The first and the fourth method did not discuss the inner boundary of footprint.

A general footprint generation approach is proposed in this paper. The footprint is divided into three different optimal problems with the same initial, path and terminal constraints. The inner boundary is solved based on a path constraint control method and dynamic inverse trajectory tracking law. The outer boundary is solved with combination of the closest approach method and the maximum crossrange method. Simulations are given and the results demonstrate the feasibility and validity of the proposed approach.

2 Footprint Problem Description

The point-mass dynamics of the re-entry vehicle over a sphere rotating Earth are described by

dimensionless equations of three dimensional motion:

$$\begin{aligned}
&\dot{r} = V\sin\gamma \\
&\dot{\theta} = V\cos\gamma\sin\psi/r\cos\phi \\
&\dot{\phi} = V\cos\gamma\cos\psi/r \\
&\dot{V} = -D - \sin\gamma/r^2 + \Omega^2 r\cos\phi(\sin\gamma\cos\phi - \cos\gamma\sin\phi\cos\psi) \\
&\dot{\gamma} = \frac{1}{V}[L\cos\sigma + (V^2 - 1/r)(\cos\gamma/r) + \\
&2\Omega V\sin\psi\cos\phi + \Omega^2 r\cos\phi(\cos\gamma\cos\phi + \sin\gamma\cos\psi\sin\phi)] \\
&\dot{\psi} = \frac{1}{V}[L\sin\sigma/\cos\gamma + V^2\cos\gamma\sin\psi\tan\phi/r - \\
&2\Omega V(\tan\gamma\cos\psi\cos\phi - \sin\phi) + \Omega^2 r\sin\psi\sin\phi\cos\phi/\cos\gamma]
\end{aligned} \tag{1}$$

Where r is the radial distance from the center of the Earth to the vehicle and normalized by the Earth radius R_0. The longitude and latitude are θ and ϕ. V is the Earth-relative velocity and normalized by $\sqrt{(g_0R_0)}$. g_0 is the gravitational acceleration magnitude on the surface of the Earth. The terms $L=\rho g_0R_0V^2S_{ref}C_L/(2mg_0)$ and $D=\rho g_0R_0V^2S_{ref}C_D/(2mg_0)$ are the aerodynamic lift and drag accelerations in g. C_L and C_D are aerodynamic coefficients. ρ is atmosphere density and S_{ref} is reference area. Here we use index atmosphere density model:

$$\rho = \rho_0 e^{-\frac{(r-1)R_0}{H}} \tag{2}$$

Where H is a constant and ρ_0 is the sea level atmosphere density with value of 1.225kg/m^3.

m is the mass and normalized by initial mass m_0. γ is flight path angle and ψ is velocity azimuth angle. The differentiation is with respect to the dimensionless time $\tau=t/\sqrt{(R_0/g_0)}$. Ω is the Earth self rotation rate normalized by $\sqrt{(R_0/g_0)}$. Bank angle σ is usually taken as control input together with AOA α.

The path constraints of entry flight are heating rate, dynamic pressure and aerodynamic load. These constraints make up the lower boundary of entry corridor. The terminal constraints are altitude r_f and velocity V_f.

Footprint is described as Fig.1. E is entry point with longitude and latitude of (θ_0, ϕ_0). The ED is the maximum downrange. The outer boundary of footprint is made up of edge AD and CD. The edge AD and CD are the point sets of maximum crossrange for each downrange EB$_i$ (B$_i$ is the point along ED). Edge AC is the inner boundary which is made up of all the end points of minimum trajectories. All the points are represented by longitude θ and latitude ϕ.

Based on the above definition of footprint, the determination of footprint involves three kinds of optimal control problem with the same initial conditions, path constraints and terminal conditions but different performance indexes. It can be converted into three sub-problems: finding point D (maximum downrange problem), determining inner boundary AC (minimum trajectory range problem), and determining edges AD and CD (maximum crossrange problem).

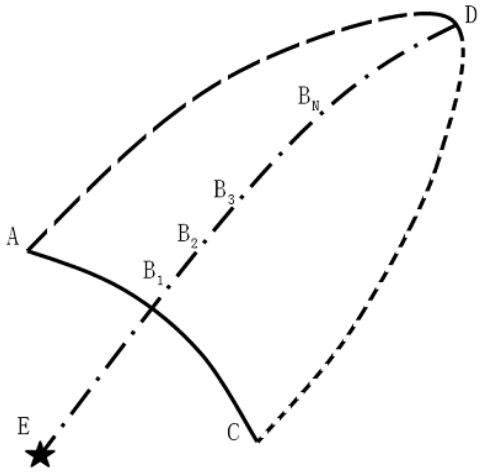

Fig. 1 Illustration of footprint

3 General Style Preferences

3.1 Maximum Downrange

The maximum downrange problem is a relatively simple one. Denoting the downrange as S_d, the optimal performance index of maximum downrange is:

$$\begin{aligned}
&\min J = \min(\cos S_d) \\
&= \min\left[\sin\phi_d\sin\phi_0 + \cos\phi_d\cos\phi_0\cos(\theta_d - \theta_0)\right]
\end{aligned} \tag{3}$$

Where $0 \leqslant S_d \leqslant \pi$. By solving this optimal problem, the maximum downrange can be found easily. Actually, the problem can be solved in another way: With predesigned nominal angle of attack, when the vehicle flies with all the aerodynamic lifting force upward in the longitudinal plane, the corresponding trajectory will have the maximum downrange for the specific angle of attack profile. The maximum downrange of footprint can be obtained by

integrating trajectory with 0° bank angle control law and maximum lift to drag ratio $L/D_{\max}$ until the energy variable e=1/r-0.5V^2 satisfying the terminal condition $e_f(V_f, r_f)$. Then the end point of trajectory is D, and the corresponding downrange is maximum downrange S_D. It can be proved that the result of this method is the same with the result from optimization.

3.2 Minimum Trajectory

Denoting S as trajectory range, the optimal performance index of minimum trajectory is:

$$\begin{aligned}\min J &= \min(S)\\ &= \min\left[-\int \frac{V\cos\gamma dV}{D+\left(\sin\gamma/r^2\right)}\right]\end{aligned} \tag{4}$$

The flight path angle γ is usually very small during re-entry and always taken approximately to 0°. So that the distance traveled along an entry trajectory is related to drag and velocity:

$$S = -\int \frac{V\mathrm{d}V}{D} \tag{5}$$

With given velocity, the minimum trajectory is corresponded to the maximum drag trajectory. So it can be obtained by flying along the lower boundary of constraints in r-V plane.

In detailed analysis (shown in the ref.[10]), it is found that path constraints of heating rate, dynamic pressure and load have a unified form in r-V plane:

$$r = k\ln V + C \tag{6}$$

k and C are constants and for different constraints they have different values. For constraints of heating rate, dynamic pressure and load the k are:

$$k_Q = 6.3H / R_0$$
$$k_q = 2H / R_0$$
$$k_n = 2H / R_0$$

The C_Q, C_q and C_n are integrate constants determined by constraint values.

It can be seen that the k for dynamic pressure and load constraints are the same and proportional with k for heating rate. That means only two of the three constraint boundaries work in r-V plane. So the lower boundary of re-entry corridor is determined by two constant parameters: C_Q, and Max$\{C_n, C_q\}$.

Based on the above conclusion of path constraint, we proposed a strategy to find the inner boundary of footprint. The entry trajectory is divided into two phases: the lower boundary tracking phase and check phase.

(1) Lower boundary tracking phase

Dynamic inverse guidance law is used to track the lower boundary of entry corridor which guarantees that this phase is the minimum range. The tracking law is [10]:

$$\sigma = \cos^{-1}\left[\frac{1}{bL}\left(\frac{\mathrm{d}^2 r_{\mathrm{ref}}}{\mathrm{d}V^2} - 2\varsigma\omega_n\frac{\mathrm{d}e}{\mathrm{d}V} - \omega_n^2 e - k_e\int e\mathrm{d}V - a\right)\right] \tag{7}$$

Where r_{ref} is the reference altitude and e is the altitude tracking error. k_e is a constant gain. ς and ω_n are damping ratio and nature frequency in velocity domain. The a and b are described in ref.[10].

To search all the points of inner boundary, the initial bank angle σ_0 can be set positive to track the lower boundary of corridor. While velocity is V_s ($V_0 \leqslant V_s \leqslant V_c$, the meaning of V_c is introduced in the following paragraph) then the sign of bank angle turns from positive to negative (for negative initial bank angle σ_0, the sign will turns from negative to positive). The V_s can be any value between (V_0,V_c). Since the sign change of bank angle effect longitudinal trajectory very slightly, the vehicle will still flight along the lower boundary with dynamic inverse guidance law.

(2) Check phase

Because of terminal constraints, the vehicle has to break from lower boundary tracking phase at certain condition. The velocity at the breaking point is denoted as V_c. After that, the vehicle flies a trajectory with the allowable maximum bank angle rate and until bank angle end up to 0. This strategy makes sure that the trajectory range is the minimum. The V_c is obtained by searching along the lower boundary. It is the point after which the vehicle flies with the above strategy and the trajectory finally satisfies the terminal constraints (V_f, r_f). It should be noted that when bank angle becomes 0, for ideal case the terminal constraints should be exactly satisfied.

A series of $V_s \in [V_0, V_c]$ are selected sequentially for both positive and negative bank

angle σ_0. Based on above two phase strategy, all the corresponding end points constitute two intersectant boundaries and the two inner half parts together make up the inner boundary AC.

Since the inner boundary is generated through trajectory planning and tracking with analytical formula and tracking law, the results could be accurate and the computation will be fast.

3.3 Maximum Crossrange

The maximum crossrange directly reflects the maneuverability of vehicle. As Fig.2 shows the downrange is S_b, the corresponding crossrange is denoted as S_m. $\angle$ EbM=90°. The optimal performance index of maximum crossrange is:

$$\begin{aligned}\min J &= \min\left(\cos S_m\right)\\ &= \min\left(\sin\phi_b \sin\phi_m + \cos\phi_b \cos\phi_m \cos\left(\theta_b - \theta_m\right)\right)\end{aligned} \tag{8}$$

Where $0 \leqslant S_m \leqslant \pi$. The maximum crossrange is denoted as S_M and the end point is M(θ_M, ϕ_M). For each downrange, there will be two maximum crossranges for both sides. And additional terminal constraint is:

$$\sin\phi_m \sin\phi_0 + \cos\phi_m \cos\phi_0 \cos\left(\theta_m - \theta_0\right) - \cos S_b \cos S_m = 0 \tag{9}$$

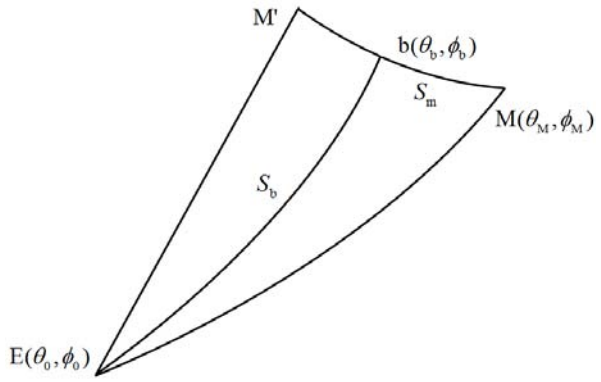

Fig. 2 The maximum crossrange with given downrange

Two methods are usually used for finding footprint outer boundary: closest-approach method with one parameter searching and maximum crossrange at prescribed downrange method with two parameters searching. These two methods are proved to be equivalence [9]. The former one is a univariate root-finding problem which can be numerical solved rapidly. But it has to set a series of virtual targets which are unreachable. These targets are chosen stochastically and usually need to adjust repeatedly to achieve good results. The latter one can provide accurate and detail information of footprint. But it is a nonlinear equations roots finding problem and usually difficult to solve.

Here we propose a new solution with benefits of both two methods.

(1)Virtual target set

First, several points are selected along the maximum downrange trajectory as B_1, B_2, …, and B_N. For each point, the corresponding maximum crossrange is calculated with prescribed downrange determined by E and B_N. Notice that the N is no need to be large (in the following simulation case, N=5 is adequate enough).

Then, the points (on solid line in Fig.3) presented for maximum crossrange are added small positives outwards and the new points (on dashed line in Fig.3) are taken as virtual targets which are definitely unreachable. The other virtual targets can be determined by interpolate.

The virtual targets obtained through above method are closed to each other. The distance between virtual targets and the actual footprint outer boundary can be controlled very small. It makes sure that the numerical computation is rapid.

(2)Trajectory optimization

For every virtual target (θ_t, ϕ_t), the closed loop bank angle guidance law is used to obtain the closest approach trajectory [8]:

$$\tan\sigma = \frac{\left(c_1\sin\phi + c_2\cos\theta\cos\phi + c_3\sin\theta\cos\phi\right)\left(1 - 1/V^2\right)}{c_1\cos\phi\sin\psi + c_2\left(\sin\theta\cos\psi - \cos\theta\sin\psi\sin\phi\right) - c_3\left(\sin\theta\sin\psi\sin\phi + \cos\theta\cos\psi\right)} \tag{10}$$

Where the three constants are:

$$c_1 = \sin\kappa$$

$$c_2 = -\tan\phi_t \sin\kappa$$

$$c_3 = \cos\kappa$$

The constant parameter κ is searched by integrating trajectory with the designed bank angle until terminal condition $e_f(V_f, r_f)$ is satisfied. The end point of the integrated trajectory is defined as (θ_f, ϕ_f). If the terminal constraint is satisfied:

$$c_1 \sin\phi_f + \left(c_2\cos(\theta_f - \theta_t) + c_3\sin(\theta_f - \theta_t)\right)\cos\phi_f = 0 \tag{11}$$

Then κ is the right one. Else κ is updated by Newton method until all the terminal constraints are enforced. When κ is found out, the corresponding trajectory is the closest approach

to the virtual target (θ_t, ϕ_t) and the end point is on the outer boundary of footprint.

Since the problem is continuous physically, the virtual targets are chosen as close as possible. So we take the optimal parameter κ of last target as the initial guess of next target. It can improve the convergence and rapidity of the searching algorithm significantly.

All the end points of the closest approach trajectories constitute the outer boundary AD and CD. With above strategy, it only needs to solve maximum crossrange for very few given downrange to obtain the virtual targets set. And then the outer boundary of footprint can be generated rapidly through the closest approach method.

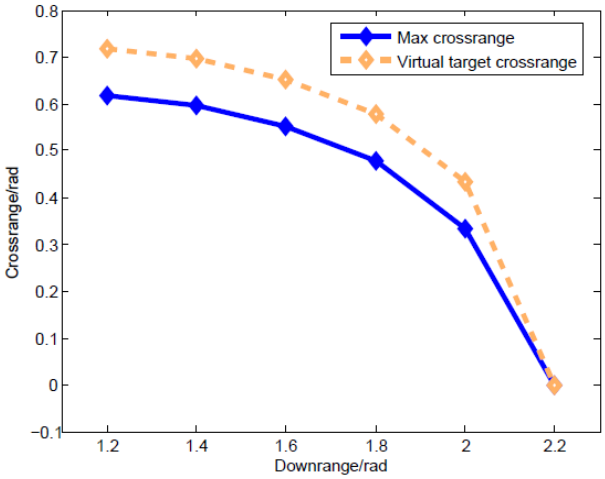

Fig. 3 Virtual targets and maximum crossrange

4 Simulation

Simulations of two cases with different initial conditions (Table.1) are given to verify the proposed method.

Table 1 Simulation condition

Variable	Case1	Case2	Meaning
h_0 km	90	80	Initial attitude
θ_0 deg	93	-157	Longitude
ϕ_0 deg	-28.255	-18.255	Latitude
V_0 m/s	7000	7000	Velocity
γ_0 deg	0	0	Flight path angle
ψ_0 deg	38.329	18.329	Velocity azimuth angle

Path constraints are the same for the two cases. The heating rate constraint is 5.2M Wa/s^2, the dynamic pressure constraint is 0.65M N/s^2, and the aerodynamic load constraint is 5g. The terminal conditions are V_f=2000m/s and r_f=35km.

(1)*Inner boundary simulation*

Take case1 for example, in Fig.4 the intersectant pink and black thick lines are the boundaries for positive and negative initial bank angle σ_0 respectively, while the thin lines are the corresponding entry trajectories. And the two half parts of pink and black thick lines (which are closer to the entry point) together constitute the inner boundary of footprint.

Fig.5 is the corresponding entry trajectories in r-V plane. Dashed lines are path constraints. Fig.6 and Fig.7 show the flight path angle and bank angle. For the most of time, flight path angle is approximately to 0 and so is the angle rate. The bank angle reverses and its absolute value is reduced to 0 with the maximum angle rate at the end of check phase.

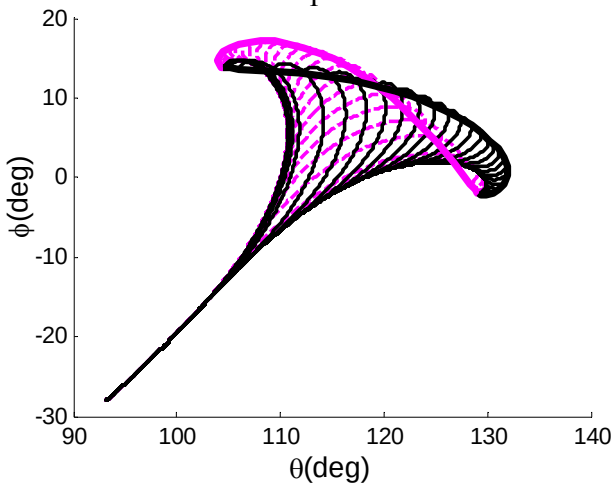

Fig. 4 Inner boundary of case1

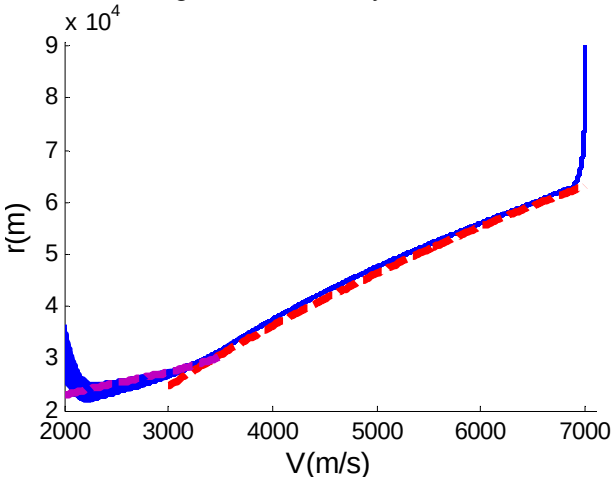

Fig. 5 Entry trajectories of case1

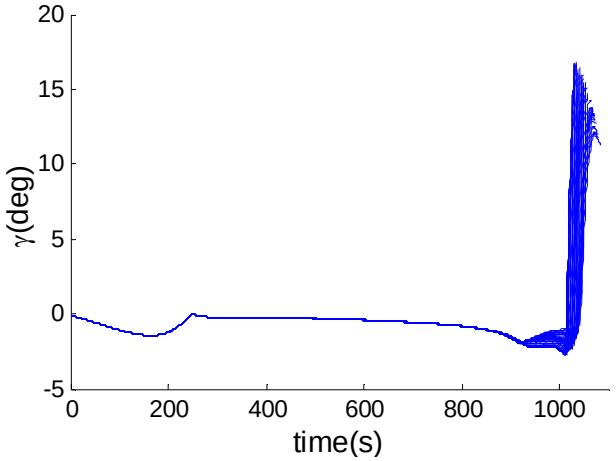

Fig. 6 Flight path angels of case1

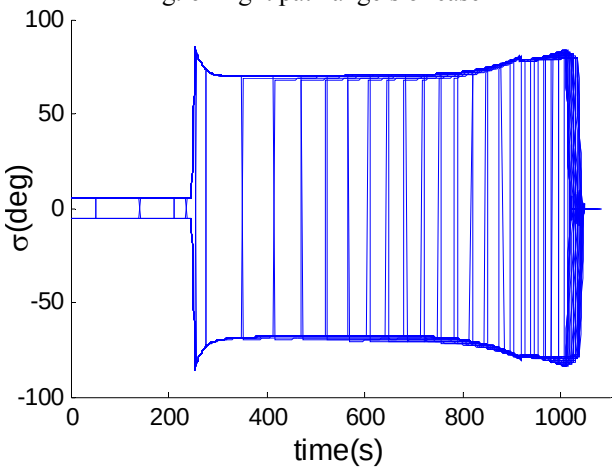

Fig. 7 Bank angles of case1

(2)*Footprint simulation*

Fig.8 is the footprints for both case1 and case2. The entry trajectories begin from different interfaces defined by latitude and longitude. The dispersed circles are virtual targets which are unreachable. The dashed lines are entry trajectories. The thick solid lines are footprints. Because of Earth rotation, the two footprints are both secund to the right hand.

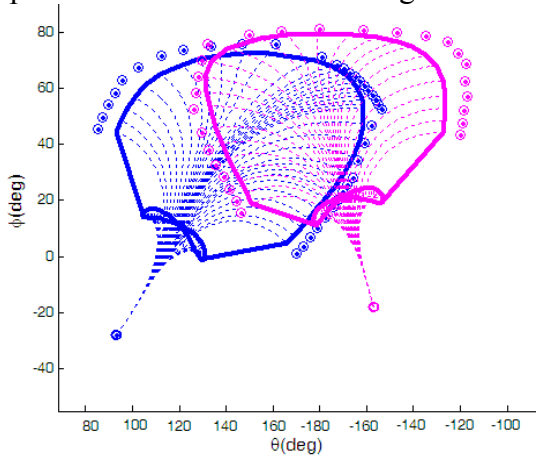

Fig. 8 Footprints for case1 and case2

5 Conclusion

A general approach for entry vehicle footprint generation is developed in this paper. It involves three different optimal control problems which are tried to be solved in fast analytical way. Based on that, the inner boundary and outer boundary of footprint can be found accurately and rapidly. The proposed methodology is an ideal tool for re-entry mission planning, analysis, and tradeoff studies on the ground.

References

[1] Vinh N X. *Optimal trajectories in atmospheric flight*. New York: Elsevier, 1981.

[2] Fahroo F, Doman D B, Ngo A D. Modeling issues in footprint generation for reusable launch vehicles. *Proceedings of the 2003 IEEE Aerospace Conference*, Big Sky, USA, March, 2003.

[3] Fahroo F, Doman D B. A direct method for approach and landing trajectory reshaping with failure effect es-timation. *AIAA Guidance, Navigation and Control Conference and Exhibit*, Providence, USA, August, 2004.

[4] Li Y, Cui N G. Optimal attack trajectory for hypersonic boost-glide missile in Maximum reachable domain. *Proceedings of the 2009 IEEE International Conference on Mechatronics and Automation*. Changchun, China, August, 2009.

[5] Li Hong-bo, Yu Meng-lun, Xiao Ye-lun. Three dimensional entry flight corridor and entry interface window about lifting reentry. *Journal of Astronautics*, Vol. 31, No. 9, pp 2059-2066, 2010

[6] Amitabh S, James A L, Kenneth D M. Landing footprint computation for entry vehicles. *AIAA Guidance, Navigation and Control Conference and Exhibit*, Providence, USA, August, 2004.

[7] James A L, Kenneth D M. Feasible trajectory generation for atmospheric entry guidance. *Journal of Guidance, Control, and Dynamics*. Vol. 30, No. 2, pp 473-481, 2007

[8] Lu P. Entry trajectory optimization with analytical feedback bank angle law. *AIAA Guidance, Navigation and Control Conference and Exhibit*, Honolulu, USA, August, 2008.

[9] Lu P, Xue S B. Rapid generation of accurate entry landing footprints. *Journal of Guidance, Control, and Dynamics*. Vol. 33, No. 3, pp 756-767, 2010.

[10] Zhang R, Li H F, Cao X D. A New Approach for Re-entry Vehicle Trajectory Planning and Guidance. *International council of the aeronautical sciences (ICAS)*. Brisbane, Australia, September, 2012.

Copyright Statement